UKnowledge

University of Kentucky
UKnowledge

Center for Applied Energy Research Faculty Publications

Center for Applied Energy Research

10-23-2015

Electrode Kinetics of Vanadium Flow Batteries: Contrasting Responses of V^{II}-V^{III} and V^{IV}-V^V to Electrochemical Pretreatment of Carbon

A. Bourke
University of Limerick, Ireland

M. A. Miller
Case Western Reserve University

R. P. Lynch
University of Limerick, Ireland

Xin Gao
University of Kentucky, xin.gao1@uky.edu

James Landon
University of Kentucky, james.landon@uky.edu

See next page for additional authors

Follow this and additional works at: https://uknowledge.uky.edu/caer_facpub

Right click to open a feedback form in a new tab to let us know how this document benefits you.

Part of the Chemical Engineering Commons, Electrical and Computer Engineering Commons, and the Materials Science and Engineering Commons

Repository Citation

Authors

A. Bourke, M. A. Miller, R. P. Lynch, Xin Gao, James Landon, J. S. Wainright, R. F. Savinell, and D. N. Buckley

Electrode Kinetics of Vanadium Flow Batteries: Contrasting Responses of V^{II}-V^{III} and V^{IV}-V^{V} to Electrochemical Pretreatment of Carbon

Electrode Kinetics of Vanadium Flow Batteries: Contrasting Responses of V^{II}-V^{III} and V^{IV}-V^{V} to Electrochemical Pretreatment of Carbon

A. Bourke,[a,b,][*] M. A. Miller,[b,][*] R. P. Lynch,[a,][**,z] X. Gao,[c,][**] J. Landon,[c,][**] J. S. Wainright,[b,][**] R. F. Savinell,[b,][***] and D. N. Buckley[a,b,][***]

[a]*Department of Physics & Energy, Materials & Surface Science Institute, University of Limerick, Limerick, Ireland*
[b]*Department of Chemical Engineering, Case Western Reserve University, Cleveland, Ohio 44106, USA*
[c]*Center for Applied Energy Research, University of Kentucky, Lexington, Kentucky 40511, USA*

Electrochemical impedance spectroscopy and cyclic voltammetry were used to investigate the electrode kinetics of V^{II}-V^{III} and V^{IV}-V^{V} in H_2SO_4 on glassy carbon, carbon paper, carbon xerogel, and carbon fibers. It was shown that, for all carbon materials investigated, the kinetics of V^{II}-V^{III} is enhanced by anodic, and inhibited by cathodic, treatment of the electrode; in contrast, the kinetics of V^{IV}-V^{V} is inhibited by anodic, and enhanced by cathodic, treatment. The potential region for each of these effects varied only slightly with carbon material. Rate constants were always greater for V^{IV}-V^{V} than for V^{II}-V^{III} except when anodized electrodes were compared, which may explain discrepancies in the literature. The observed effects are attributed to oxygen-containing functional-groups on the electrode surface. The considerable differences between the potentials at which enhancement of V^{II}-V^{III} and inhibition of V^{IV}-V^{V} occur indicates that they do not correspond to a common oxidized state of the electrode. Likewise inhibition of V^{II}-V^{III} and enhancement of V^{IV}-V^{V} do not correspond to a common reduced state of the electrode. It is possible that enhancement of both V^{II}-V^{III} and V^{IV}-V^{V} is due to the same (active) state of the electrode.

There is considerable interest in vanadium flow batteries (VFBs), also known as vanadium redox flow batteries (VRFBs or VRBs), for storage of electrical energy particularly in conjunction with renewable energy sources such as wind and solar.[1–6] Active areas of research include cell design and modelling,[7–9] performance and state-of-charge monitoring,[10–16] coulombic and energy efficiencies,[5,17,18] electrolytes,[11–16,19,20] membranes,[4,21] and electrodes.[22–56] Cells typically have porous carbon electrodes and electrode performance can depend strongly on electrode treatment. Various electrochemical,[22–27,36–41] chemical,[36,40,43,44] and thermal[45–49] treatments have been reported. These treatments often have the effect of oxidizing or reducing the surface, and the influence of surface oxygen species on electrochemical kinetics at carbon electrodes is recognized,[22,57–60] although often not well understood.

Thermal[45–49] and chemical[36,40,43,44] treatments of electrodes for VFBs have been tested on a range of carbon-based electrodes and, in general, these treatments result in higher activities of the electrode toward the vanadium redox reactions. There are also a number of reports of the effect of electrochemical treatment of electrodes. Anodic treatment of carbon felt was reported[22,36] to cause a decrease in the kinetic rates of the V^{IV}-V^{V} redox couple. In contrast, there are also reports of enhancement of V^{IV}-V^{V} kinetics after electrochemical oxidation[38–41] (of graphite and carbon felt electrodes) and of V^{II}-V^{III} kinetics after potential cycling[61] (of highly-oriented-pyrolytic-graphite and glassy carbon electrodes). However, in considering the effects of anodization on a carbon surface it must be borne in mind that carbon can corrode at anodic potentials and that this can sometimes lead to roughening of the surface with a consequent enhancement of electrode current. On the other hand, cathodic treatment of an electrode consisting of graphene oxide on a glassy-carbon substrate was reported[37] to cause an increase in the kinetic rates of both V^{IV}-V^{V} and V^{II}-V^{III} redox

couples. It has also been reported[62] that after hydrogen evolution had occurred on a graphite electrode that the kinetic rate of the V^{II}-V^{III} redox couple was decreased. The vanadium redox reactions are clearly very sensitive to the chemistry of the carbon surface.

The kinetics of both V^{II}-V^{III} and V^{IV}-V^{V} redox couples have been studied for a range of different carbon materials using a variety of techniques, and it is clear that the kinetic rates depend strongly both on the type of carbon used and on the preparation of the electrode surface.[29,46,50–52] Generally, the kinetics are reported[17,28–33] to be faster for V^{IV}-V^{V} than for V^{II}-V^{III}; however there are also reports[34,35,63] that V^{IV}-V^{V} has slower kinetics than V^{II}-V^{III}. Table I shows a comparison of kinetic rate metrics for a range of carbon materials for both the V^{II}-V^{III} and V^{IV}-V^{V} reactions. It is clear from this table that even on the same electrode material, e.g. glassy carbon, and for the same

Table I. Comparison of the kinetic rate constants k_o at the electrodes indicated for both V^{II}-V^{III} and V^{IV}-V^{V}. Also calculated is the rate ratio k_{45}/k_{23} (k_{45} and k_{23} represent, respectively, the values of k_o for V^{IV}-V^{V} and V^{II}-V^{III}).

| Electrode Material | Reference | k_o ($\times 10^{-6}$ cm s^{-1}) | | Rate Ratio |
		V^{II}-V^{III}	V^{IV}-V^{V}	k_{45}/k_{23}
Glassy carbon	29,30	17	750	44
	50	54	13	0.24
	28	1.0	(150)[a]	150
Carbon Paper	31	(30.9)[a]	(1360)[a]	44
	50	1130	1040	0.92
Pyrolytic Graphite	51	550	130	0.24
	50	35	517	15
Felt	45	15.4	18.3	1.2
Plastic Formed Carbon	51	530	850	1.6
Graphite Reinforced Carbon	35	9700	5000	0.52

[a]Rate constants k_o were calculated from the reported data for the exchange current density assuming a symmetry factor α of 0.5.

electrolyte species, e.g. V^{II}-V^{III}, the kinetic rate metrics reported vary by over an order of magnitude from author to author. Also calculated in Table I is the rate ratio (i.e. the ratio of the kinetic rate constant k_o for V^{IV}-V^{V} oxidation-reduction to that for V^{II}-V^{III}). These ratios vary from 0.24 to 150. Thus, not only is there a discrepancy as to the magnitude of the relative activities but there is also a discrepancy[7] as to which half-cell has faster kinetics. Thus, the electrode kinetics of these vanadium redox couples, which are the basis of the VFB, require further investigation.

We have reported[22–27] preliminary results showing that electrochemical treatment of carbon electrodes can have very significant effects on electrode kinetics. These include enhancement of V^{II}-V^{III} kinetics and inhibition of V^{IV}-V^{V} kinetics by anodic treatment; and enhancement of V^{IV}-V^{V} and inhibition of V^{II}-V^{III} by cathodic treatment. We examined in detail[22] the effects of electrode pretreatment on the kinetics of V^{IV}-V^{V} on several types of carbon electrodes using cyclic voltammetry and electrochemical impedance spectroscopy. Our results demonstrated that, in all cases, pronounced activation of electrodes typically occurs at treatment potentials more negative than ∼+0.1 V and pronounced deactivation at treatment potentials more positive than ∼+0.7 V. The activation and deactivation effects are observed regardless of whether vanadium is present in the electrolyte during electrode treatment and are attributed to oxygen-containing functional groups on the electrode surface.

In this paper we report a detailed comparison of the contrasting effects on the kinetics of V^{II}-V^{III} and V^{IV}-V^{V} of both anodic and cathodic electrode treatments for several carbon materials and show that an understanding of these effects can explain many of the discrepancies in the literature.

Experimental

Glassy carbon was supplied by Tokai Carbon, carbon paper (SpectraCarb 2050L) by Fuelcellstore, and carbon xerogel[64–67] by the University of Kentucky; fibers were extracted from carbon felt (TS5345) supplied by Graftech.

Glassy-carbon electrodes were constructed by contacting the back of the carbon coupon to a copper wire using carbon conductive adhesive (Leit-CCC from SPI Supplies). The contact was isolated from the electrolyte with epoxy (Hardman) so that only the carbon surface of interest was exposed. The wire was sealed into glass tubing with epoxy.

A similar contact configuration was also used in the construction of electrodes of other carbon materials. In the case of the porous materials (carbon paper and carbon xerogel), the contact was isolated from the electrolyte by filling a section of the porous material with lacquer/epoxy and sealing into glass tubing with epoxy. Again, only the carbon surface of interest was exposed to the electrolyte.

Single-fiber micro-electrodes were constructed by extracting a fiber from bulk graphite felt. The fiber was mounted across a raised glass platform and each end of the fiber was connected to a separate copper wire using carbon or silver (Silver Paste Plus from SPI Supplies) conductive adhesives. The contacts were isolated from the electrolyte using epoxy and glass. The wires were sealed into glass tubing with epoxy.

A conventional three-electrode cell configuration was used employing a platinum counter electrode and saturated Hg/Hg_2SO_4 reference electrode to which all potentials were referenced. The cell was thermostatted at 25°C and the electrolyte deaerated by purging with nitrogen. V^{IV} electrolyte solutions (1.5 mol dm^{-3} vanadium and 4.5 mol dm^{-3} sulfate) were prepared using sulfuric acid and vanadyl sulfate ($VOSO_4$) supplied by Sigma Aldrich. V^{II} and V^{V} solutions were obtained by reducing or oxidizing the V^{IV} solution in a flow cell. These were then used to prepare mixed electrolyte solutions (1:1 V^{IV}-V^{V} and 1:1 V^{II}-V^{III}). Air exposure of V^{II} solutions and V^{II}-V^{III} mixtures was avoided as far as possible and all experiments were carried out under nitrogen-sparged conditions. A Metrohm Autolab (model PGSTAT100) Electrochemical Workstation interfaced to a computer was employed for cell parameter control and for data acquisition.

Cyclic voltammograms (CVs) were run continuously at 50 mV s^{-1}, beginning at the rest potential with switching potentials of −1.25 V and −0.6 V, for the V^{II}-V^{III} system, and 0.8 V and 0.2 V, for the V^{IV}-V^{V} system, until steady-state curves were obtained. The steady-state CV (typically the 10th cycle) was used as a diagnostic of electrode activity. Electrochemical impedance spectroscopy (EIS) measurements were carried out at the rest potential with an a.c. amplitude of 10 mV from 20 kHz to 0.2 Hz, and data were analyzed using a Randles equivalent circuit so as to calculate charge transfer resistances.

In this work, the effect of electrochemical treatment potential was investigated in detail in a series of experiments that will be described in the results section. Before each experiment, electrodes were subjected to a normalization treatment[22] typically three cycles, each of 60 s at a cathodic potential of −2.0 V (for experiments in V^{II}-V^{III} electrolyte) or −0.9 V (for experiments in V^{IV}-V^{V} electrolyte) and 60 s at an anodic potential of +1.5 V. The purpose of this normalization treatment was to minimize any effect of electrode history. Newly-constructed electrodes underwent a number of normalization treatments before use in experiments (i.e. all electrodes were initially aged).

Results and Discussion

Effect of electrode treatment on V^{II}-V^{III} and V^{IV}-V^{V} kinetics.— The effects of both anodic and cathodic treatment of a glassy-carbon electrode on the electrode kinetics of both V^{II}-V^{III} and V^{IV}-V^{V} were investigated by electrochemical impedance spectroscopy (EIS) and cyclic voltammetry.

Typical results for V^{II}-V^{III} are shown in Fig. 1a where EIS was used to monitor electrode kinetics on the same glassy-carbon electrode under the same conditions but after two different treatments. Curve A was obtained after the electrode had been anodically treated at +1.5 V for 60 s while Curve C was obtained after it had subsequently been cathodically treated at −2.0 V for 60 s. Clearly, the charge transfer resistance is much larger in C than in A, indicating that the kinetics of V^{II}-V^{III} are inhibited by cathodic treatment. Subsequent anodic treatment at +1.5 V for 60 s again gave a curve similar to A. The behavior of the electrode could be "toggled" repeatedly in this way between a reduced state and an oxidized state with corresponding curves similar to C and A respectively.

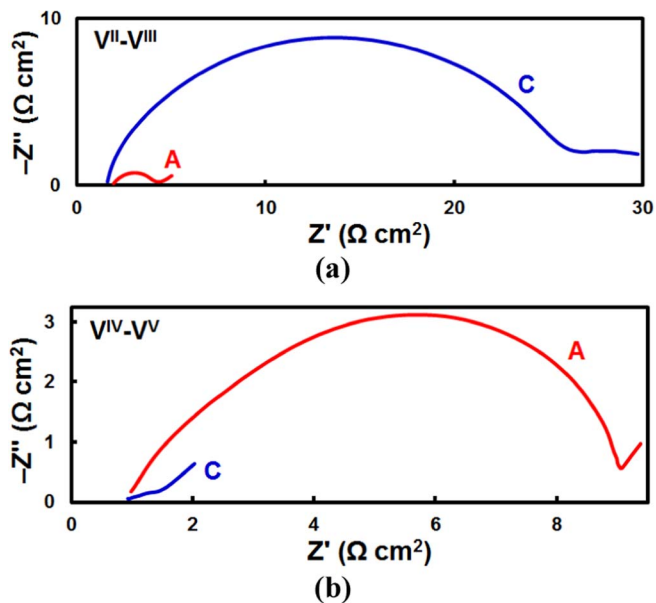**Figure 1.** Comparison of Nyquist plots for a glassy-carbon electrode after anodic and cathodic treatments in (a) a V^{II}-V^{III} electrolyte and (b) a V^{IV}-V^{V} electrolyte. Curve A was obtained after anodic treatment at +1.5 V for 60 s. Curve C was obtained after cathodic treatment at (a) −2.0 V and (b) −0.9 V for 60 s. EIS were run at the rest potential with an a.c. amplitude of 10 mV.
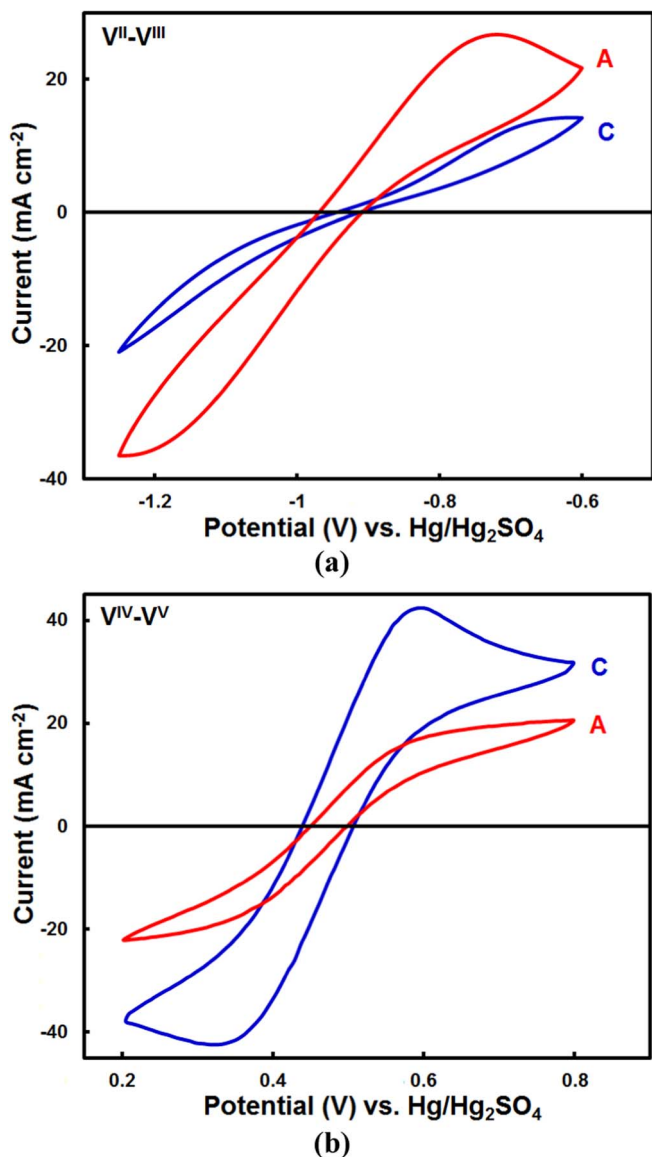
Figure 2. Comparison of CVs of a glassy-carbon electrode after anodic and cathodic treatments in (a) a V^{II}-V^{III} electrolyte and (b) a V^{IV}-V^V electrolyte. Curve A shows the steady-state CV after anodic treatment at +1.5 V for 60 s. Curve C shows the steady-state CV after cathodic treatment at −2.0 V for 60 s. The scan rate was 50 mV s^{-1}.

Figure 3. (a) Nyquist plots and (b) CVs for a glassy-carbon electrode in a V^{II}-V^{III} electrolyte after anodic treatment at the potentials indicated. Before anodic treatment in each case the electrode was cathodically pretreated at −2.0 V for 60 s. In both (a) and (b), the broken line shows a typical (baseline) curve for the cathodically pretreated electrode. After each anodic treatment, the electrode was allowed to rest at open circuit for 60 s after which EIS measurements were made with an a.c. amplitude of 10 mV followed by CVs at 50 mV s^{-1}. The 10th CV (steady state) is shown in each case. Normalization treatment, described in the Experimental section, was carried out between experiments. Selected frequencies are indicated in the Nyquist plots: 100 Hz ○, 10 Hz △, and 1 Hz ◇.

Corresponding results[22] for V^{IV}-V^V are shown in Fig. 1b. However, in sharp contrast with Fig. 1a, the charge transfer resistance is much smaller in C (after cathodic treatment) than in A (after anodic treatment) indicating that the kinetics of V^{IV}-V^V are enhanced by cathodic treatment.

Fig. 2 shows results of experiments similar to those in Fig. 1 except that in this case cyclic voltammetry was used to monitor the reaction rates. Typical results for V^{II}-V^{III} are shown in Fig. 2a. The shapes of the voltammograms in Fig. 2 are complex. However, we restrict our focus to a narrow potential window close to the rest potential, where linear kinetics should predominate. Clearly, in this region the currents are much smaller in C (after cathodic treatment) than in A (after anodic treatment), confirming the results in Fig. 1a that the kinetics of V^{II}-V^{III} are inhibited by cathodic treatment. Corresponding results for V^{IV}-V^V are shown in Fig. 2b. In this case, the currents close to the rest potential are much larger in C than in A confirming the results in Fig. 1b that the kinetics of V^{IV}-V^V are enhanced by cathodic treatment.
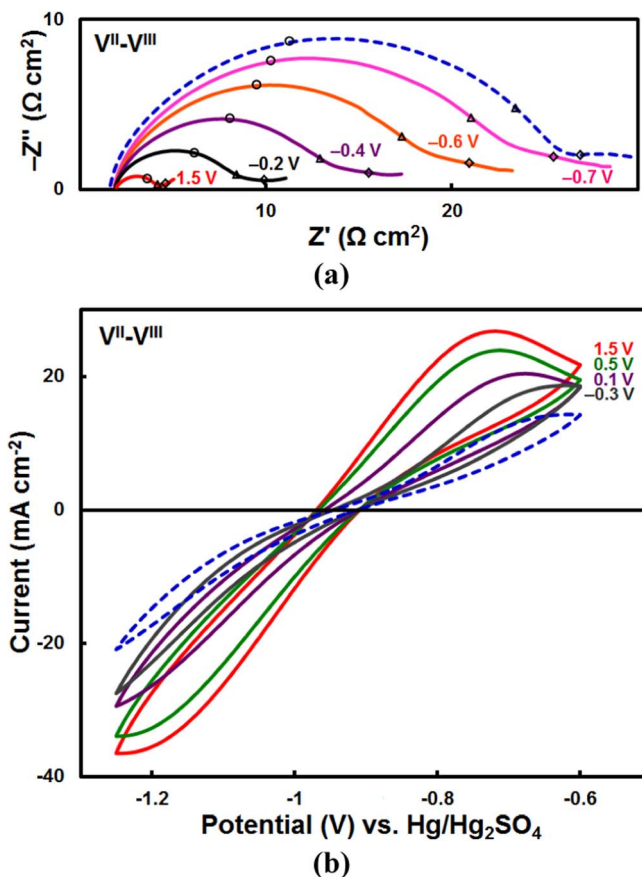
The reproducibility of these effects was excellent. Both EIS and CV experiments showed that alternate cathodization and anodization of the electrode repeatedly toggled its behavior as described, with cathodization always leading to inhibition of V^{II}-V^{III} and enhancement of V^{IV}-V^V. Similar effects were observed when the electrode was anodically or cathodically treated at other potentials.

Thus, the results obtained in V^{II}-V^{III} electrolyte (Figs. 1a and 2a) are in direct contrast to those obtained in V^{IV}-V^V electrolyte (Figs. 1b and 2b): the rates of the V^{II}-V^{III} reactions were inhibited by cathodic treatment, while the rates of the V^{IV}-V^V reactions were enhanced by cathodic treatment.

Effect of treatment potential.— Similar effects to those illustrated in Figs. 1 and 2 were observed when the electrode was anodically or cathodically treated at other potentials. The reproducibility of these effects was excellent at all treatment potentials investigated.

To examine the effect of anodic treatment potential on V^{II}-V^{III} kinetics, a series of experiments was carried out. In each experiment an electrode which had initially been treated cathodically was then treated at a selected anodic potential. Typical results are shown in Fig. 3. The broken line in Fig. 3a shows a typical Nyquist plot (baseline) of a cathodically treated electrode and the solid lines show plots after treatment at selected anodic potentials. It can be seen that
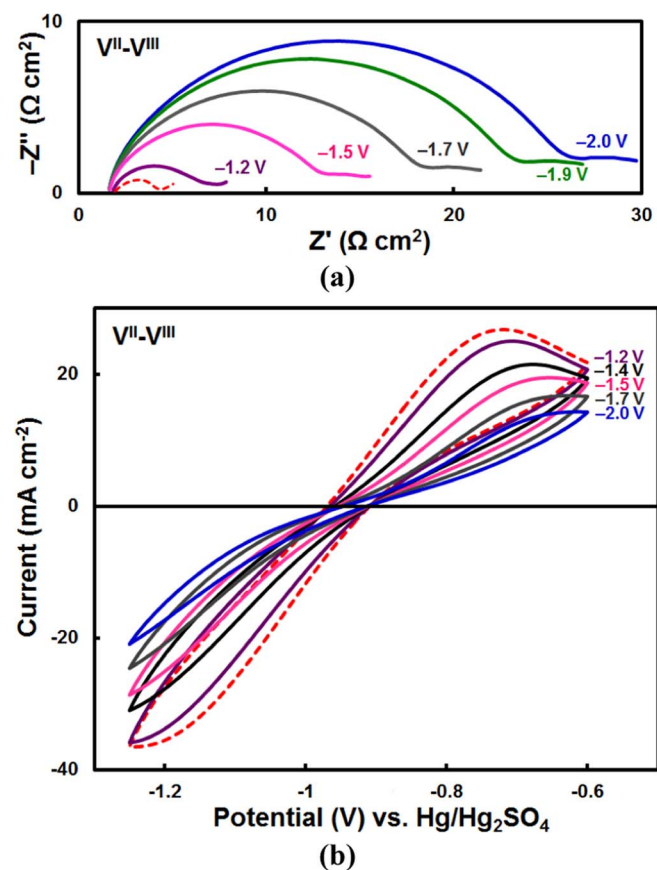
Figure 4. (a) Nyquist plots and (b) CVs for a glassy-carbon electrode in a V^{II}-V^{III} electrolyte after cathodic treatment at the potentials indicated. Before cathodic treatment in each case the electrode was anodically pretreated at 1.5 V for 60 s. In both (a) and (b), the broken line shows a typical curve (baseline) of an anodically pretreated electrode and the solid lines show curves after treatment at selected cathodic potentials. The methodology was similar to that used for the results in Fig. 3.

Figure 5. Rate constants (open circles) from EIS results in Figs. 3a and 4a, and CV currents (closed circles) from Figs. 3b and 4b plotted against anodic (A) and cathodic (C) treatment potential (for a glassy-carbon electrode in a 1:1 V^{II}-V^{III} electrolyte). Each CV current shown is the average of the absolute values of current at +25 mV and −25 mV with respect to the rest potential.

as the treatment potential is made progressively more positive, the semi-circle diameters in the subsequent Nyquist plots are progressively smaller (decreased charge-transfer resistance) indicating progressively increased activation of the electrode.

Similarly, the broken line in Fig. 3b shows a typical CV (baseline) of a cathodically treated electrode and the solid lines show CVs after treatment at selected anodic potentials. It can be seen that as the treatment potential is made progressively more positive, the currents in the subsequent CVs are progressively larger indicating progressively increased activation of the electrode.

The effect of cathodic treatment potential on V^{II}-V^{III} kinetics was investigated in a similar series of experiments; typical EIS results from this series of experiments are shown in Fig. 4a and CV results in Fig. 4b. In each case, the broken line shows a typical curve (baseline) of an anodically treated electrode, and the solid lines show curves after treatment at selected cathodic potentials. Clearly, as the treatment potential is made progressively more negative, the charge-transfer resistances in the Nyquist plots are progressively larger and the currents in the corresponding CVs are progressively smaller indicating progressively increased deactivation of the electrode.

The activity of the electrode after treatment at a given potential was quantitatively estimated using metrics from both EIS (Figs. 3a and 4a) and CV measurements (Figs. 3b and 4b). For the EIS, the metric was the electrochemical rate constant k_o estimated[68] from the charge transfer resistance; for the CVs, the metric was the average of the absolute values of current at +25 mV and −25 mV (with respect to the rest potential). Results for each metric are plotted against treat-
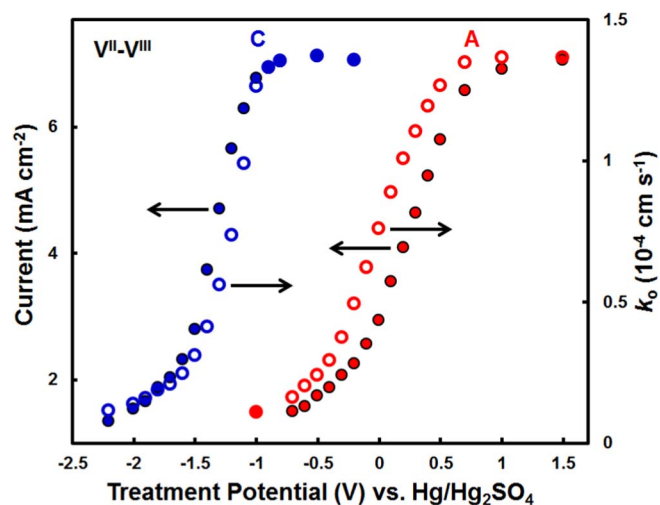
ment potential in Fig. 5. The changes in activity are large; e.g., the value of k_0 after anodic treatment at 1.5 V is greater by a factor of ~10 than that after cathodic treatment at −2 V. It can be seen that there is good agreement between the two metrics with regard to the potential region in which activation and deactivation of the electrode occurs. For anodic treatment (A), at potentials more positive than ~−0.4 V the activity begins to increase; this trend continues as the potential is made more positive with a rapid increase in activity between −0.4 V and +0.5 V until the effect appears to approach saturation at ~+1.0 V. For cathodic treatment (C), at potentials more negative than ~−0.9 V the activity begins to decrease; this trend continues as the potential is made more negative with a rapid decrease in activity between −1.0 V and −1.5 V until the effect appears to approach saturation at ~−2.0 V.

There is a considerable shift in potential between the activation (A) and deactivation (C) curves in Fig. 5. The average potential of the 50% point on the activation curve is ~0.1 V while the corresponding potential on the deactivation curve is ~−1.3 V, a hysteresis of ~1.4 V.

The effect of treatment potential on V^{IV}-V^V kinetics was also investigated.[22] Results for both anodic and cathodic treatment of glassy carbon, over a similar range of treatment potential to that in Fig. 5 for V^{II}-V^{III}, are plotted for V^{IV}-V^V in Fig. 6. The changes in activity are large; e.g., the value of k_0 after cathodic treatment at −1.0 V is greater by a factor of ~10 than that after anodic treatment at 1.6 V. It can be seen that there is good agreement between the two metrics with regard to the potential region in which activation and deactivation of the electrode occurs. For anodic treatment (A), as the potential is made progressively more positive than ~+0.7 V, the electrode activity progressively decreases. For cathodic treatment (C), at potentials more negative than ~+0.4 V the activity begins to increase; this trend continues as the potential is made more negative with a rapid increase in activity between +0.1 V and −0.3 V until the effect appears to approach saturation at ~−0.6 V. The average potential of the 50% point on the activation curve is ~−0.3 V while the corresponding potential on the deactivation curve is ~0.9 V, a hysteresis of 1.2 V. These results are in direct contrast to those observed for the V^{II}-V^{III} system in Fig. 5.

Other carbon materials.— The effects of electrode treatment on the kinetics of V^{II}-V^{III} and V^{IV}-V^V were also investigated for other carbon materials. Materials examined included carbon paper, carbon xerogel, and carbon fibers (obtained from typical felt used in
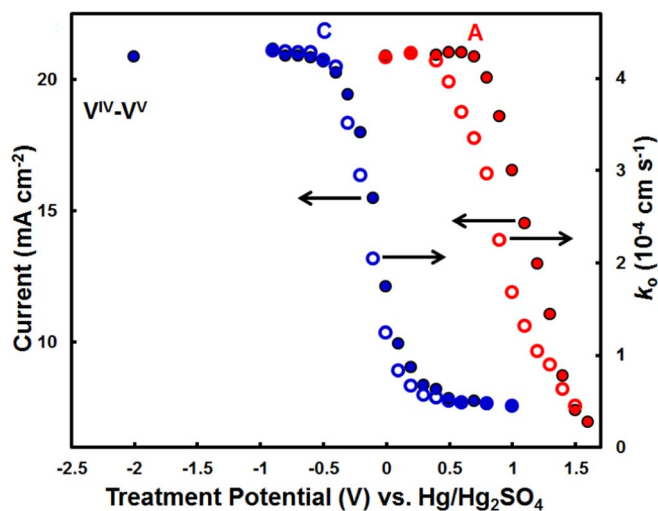
Figure 6. Rate constants (open circles) from EIS results and CV currents (closed circles) plotted against anodic (A) and cathodic (C) treatment potential for a glassy-carbon electrode in a V^{IV}-V^V electrolyte. The experiments were carried out similarly to those for Fig. 5.
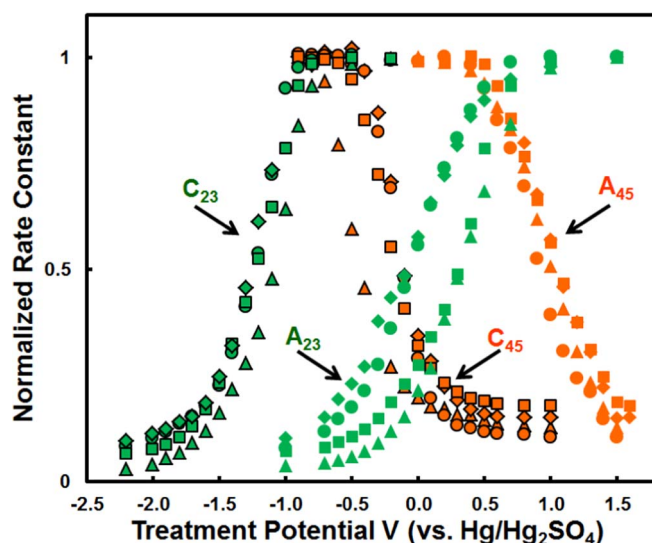

Figure 7. Normalized rate constant plotted against treatment potential for four types of carbon. Data for both anodic (A) and cathodic (C) treatments are shown for both V^{II}-V^{III} (A_{23} and C_{23}) and V^{IV}-V^V (A_{45} and C_{45}). The materials shown are: glassy carbon ●, carbon paper ▲, carbon xerogel ■, and carbon fiber ♦. Rate constants k_o are normalized to their maximum value k_{max} in each case (i.e. k_o/k_{max}). The experiments were carried out as described earlier for Figs. 5 and 6.

commercial flow batteries). The detailed effects of treatment potential on each type of carbon electrode were investigated for both anodic and cathodic treatments in series of experiments similar to those described above for glassy carbon.

The results are summarized in Fig. 7 where the normalized rate constant after both cathodic (C) and anodic (A) treatment is plotted against treatment potential for both V^{II}-V^{III} (C_{23} and A_{23}) and V^{IV}-V^V (C_{45} and A_{45}). It can be seen that all four carbons behave in a similar manner: in all cases, anodic treatment results in enhancement of V^{II}-V^{III} and inhibition of V^{IV}-V^V while cathodic treatment results in inhibition of V^{II}-V^{III} and enhancement of V^{IV}-V^V. Furthermore, it can be seen that in each case (A_{23}, A_{45}, C_{23} and C_{45}) activation or deactivation occurs over a similar range of potential for all four carbons. The values of k_o for both V^{II}-V^{III} and V^{IV}-V^V after maximum anodic treatment (k_{an}) and maximum cathodic treatment (k_{cat}) are listed in Table II for all four carbons investigated. The ratio k_{an}/k_{cat}, which we call the anodic treatment factor (ATF), is also shown in each case. It can be seen that in all cases the ATF is >1 for V^{II}-V^{III}, ranging from 8.87 for carbon fiber to 24.6 for carbon paper. In contrast, in all cases the ATF is <1 for V^{IV}-V^V, ranging from 0.104 for glassy carbon to 0.212 for carbon fiber.

In all cases, the electrodes could be repeatedly and reproducibly toggled between activated and deactivated states by the corresponding anodic and cathodic treatment, just as was the case with glassy carbon. The results showed that all of these materials (carbon paper, carbon xerogel, and the constituent fibers of carbon felt) behaved similarly to glassy carbon.

In summary, for four different carbons and based on two different techniques (EIS and CV) in each case, our results clearly show that the kinetics of V^{II}-V^{III} is enhanced by anodic, and inhibited by cathodic, treatment of the electrode; in contrast, the kinetics of V^{IV}-V^V

is inhibited by anodic, and enhanced by cathodic, treatment. Thus, the results are quite general for many types of carbon and, regardless of the underlying mechanism, the conclusions are most important in the context of the VFB. Enhancement factors vary somewhat with electrode material, but in all cases are quite large, ranging from ∼10 to ∼25 for V^{II}-V^{III} and from ∼5 to ∼10 for V^{IV}-V^V (based on the ratio of the measured values of k_0). Because of the size of these effects, they are clearly evident in all cases, regardless of the detailed electrode kinetics of each of the two couples on the particular carbon material. Further work needs to be done to more precisely characterize the kinetics and mechanism for each of the couples. It is now clear from our work that such studies will need to take careful account of the effects of electrode treatment.

Comparison of V^{II}-V^{III} and V^{IV}-V^V.— As discussed in the introduction, there are conflicting reports in the literature as to which electrode kinetics is faster, V^{II}-V^{III} or V^{IV}-V^V. It is clear from the above that comparison is complicated by the strong and contrasting effects of electrode treatments for the two systems. However, as will be shown in this section, the V^{IV}-V^V reaction is, in general, faster than the V^{II}-V^{III} reaction for any given carbon material.

Plots of rate constants for the two couples at glassy-carbon are compared in Fig. 8. It can be seen that the rate of V^{IV}-V^V after cathodic activation (C_{45}) is ∼3 times greater than that of V^{II}-V^{III} after anodic activation (A_{23}). Likewise the rate of V^{IV}-V^V after anodic deactivation (A_{45}) is ∼3 times greater than that of V^{II}-V^{III} after cathodic

Table II. Comparison of rate constants k_o after maximum anodic treatment (k_{an}) and maximum cathodic treatment (k_{cat}) obtained from EIS results for the electrodes indicated. The anodic treatment factor (ATF = k_{an}/k_{cat}) is also shown in each case. Results for both V^{II}-V^{III} and V^{IV}-V^V are shown (from Fig. 5 and Fig. 6, respectively, in the case of glassy carbon).

	V^{II}-V^{III}			V^{IV}-V^V		
Electrode Material	k_{an} ($\times 10^{-6}$ cm s^{-1})	k_{cat} ($\times 10^{-6}$ cm s^{-1})	ATF	k_{an} ($\times 10^{-6}$ cm s^{-1})	k_{cat} ($\times 10^{-6}$ cm s^{-1})	ATF
Glassy Carbon	136	13.8	9.86	44.8	430	0.104
Carbon Paper	27.7	1.13	24.6	28.1	160	0.176
Carbon Xerogel	369	28.2	13.1	220	1183	0.186
Fiber	76.3	8.60	8.87	36.0	170	0.212

Table III. Rate of V^{IV}-V^V relative to V^{II}-V^{III} (k_{45}/k_{23}) for the four possible comparisons of electrode treatment (listed in Columns 1 and 2): the effects of the treatments (activation or deactivation) are shown in brackets. In each case the ratio of the value of k_{45} measured after the treatment indicated in Column 1 to the value of k_{23} measured after the treatment in Column 2 is shown for each carbon material; k_{45} and k_{23} represent, respectively, the values of k_o for V^{IV}-V^V and V^{II}-V^{III}. Anodic treatment was for 60 s at +1.5 V; cathodic treatment was for 60 s at −0.9 V (for V^{IV}-V^V) or −2.0 V (for V^{II}-V^{III}).

|		Rate Ratio (k_{45}/k_{23})			
Treatment for V^{IV}-V^V	Treatment for V^{II}-V^{III}	Glassy Carbon	Carbon Paper	Carbon Xerogel	Fiber
Cathodization (Activation)	Anodization (Activation)	3.16	5.78	3.21	1.80
Anodization (Deactivation)	Cathodization (Deactivation)	3.25	24.9	7.80	2.37
Cathodization (Activation)	Cathodization (Deactivation)	31.2	142	42.0	15.9
Anodization (Deactivation)	Anodization (Activation)	0.33	1.01	0.60	0.27
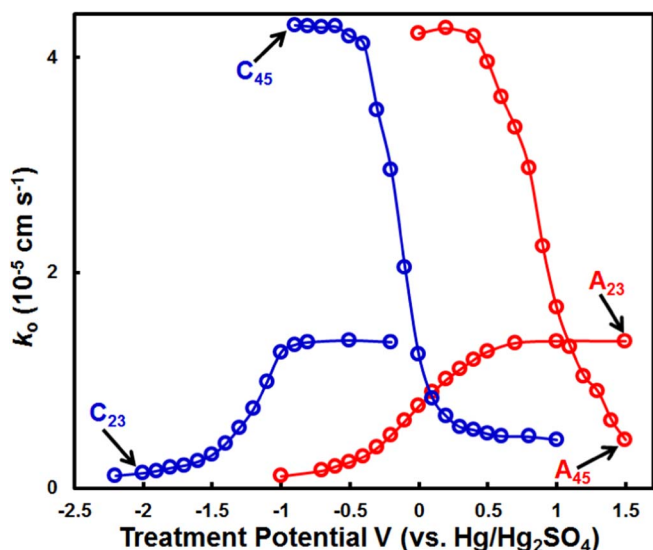
Figure 8. Comparison of rate constants for V^{II}-V^{III} (Fig. 5) with those for V^{IV}-V^V (Fig. 6). A_{23} and C_{23} correspond to V^{II}-V^{III} after, respectively, anodic and cathodic treatment of the electrode; similarly A_{45} and C_{45} correspond to V^{IV}-V^V.

deactivation (C_{23}).[d] It is also clear that on a cathodically treated electrode the rate is much larger (×31) for V^{IV}-V^V than for V^{II}-V^{III} (compare C_{45} and C_{23} in Fig. 8). Only on an anodically treated electrode is the rate of V^{II}-V^{III} greater than that of V^{IV}-V^V (compare A_{23} and A_{45} in Fig. 8). CV results for V^{II}-V^{III} and V^{IV}-V^V are compared in the Appendix.

Rate ratios of V^{IV}-V^V to V^{II}-V^{III} are similarly compared in Table III for all of the four carbon materials investigated. It can be seen that the rate of V^{IV}-V^V is always greater than that of V^{II}-V^{III} except (in some cases) on an anodized electrode. This analysis highlights that when V^{IV}-V^V and V^{II}-V^{III} are "legitimately" compared (i.e. when both electrodes are activated or both are deactivated), the rate of V^{IV}-V^V is always greater. Only on an anodically treated electrode may the rate of V^{II}-V^{III} be greater, but this may be regarded as not being a legitimate comparison because anodization enhances V^{II}-V^{III} and inhibits V^{IV}-V^V.

The foregoing may explain reports in the literature[34,35,63] that the kinetics of V^{II}-V^{III} is faster than that of V^{IV}-V^V. It may also explain the surprisingly large variation in the ratio of rate constants (see Table I) for V^{IV}-V^V and V^{II}-V^{III} where both measurements were made on the same electrode in the same study. Thus, as can be seen from Table III, the rate ratio for a particular material may vary by two orders of magnitude depending on the particular pair of treatments

compared. In the absence of clear data for the contrasting effects of anodization and cathodization on V^{II}-V^{III} and V^{IV}-V^V kinetics, such as we report in this paper, it would be reasonable to compare electrodes which had been pretreated in a similar manner. However, as we now know, very different results would be obtained depending on whether anodic or cathodic pretreatment of the electrode was chosen. It is thus unsurprising that there are conflicting reports[17,28–35] in the literature as to which VFB electrode has slower kinetics.

In fact, the effect of electrode treatment on kinetics is often as significant as the effect of carbon material, as seen in Table II. For example, the rate constant for V^{II}-V^{III} on anodized carbon xerogel is 13.3 times greater than that on anodized carbon paper; by comparison the enhancement factor due to anodization is 13.1 for the carbon xerogel and 24.6 for the carbon paper.

Nature of the effects of anodization and cathodization on the electrode.— The effects of electrochemical pretreatment of carbon electrodes on the kinetics of a number of other redox couples has been reported.[60,69–72] For most couples, anodic treatment of a carbon electrode inhibits the redox reaction while cathodic treatment enhances it. Thus, the effects of electrode treatment on V^{IV}-V^V are consistent with results for other systems but the contrasting effects on V^{II}-V^{III} are remarkable.

It might be suggested that the enhancement of V^{II}-V^{III} simply reflects surface roughening due to corrosion of carbon. Indeed, we have observed some increase in the area of newly fabricated electrodes during anodization at higher potentials, but after electrodes have been subjected to a number of cathodic and anodic treatments, a steady state is reached. In contrast, electrodes which show enhanced activity for V^{II}-V^{III} after anodic treatment always return to their original lower level of activity on subsequent cathodic treatment. This activation and deactivation by alternate anodization and cathodization may be continued indefinitely. Furthermore, the observed degree of activation and deactivation is quantitatively related to the treatment potential with excellent reproducibility. Thus, although surface roughening effects are commonly found to cause enhancement of electrochemical activity, they cannot explain the highly reversible behavior observed in the present study. This is further supported by the observation that anodic activation of the electrode for V^{II}-V^{III} occurs at less positive potentials (i.e. milder corrosion conditions) than anodic deactivation of the electrode for V^{IV}-V^V (see Table IV).

We proposed earlier[22] that oxygen-containing species, known to occur on the surface of carbon electrodes, are responsible for the observed effects of cathodic and anodic treatment of electrodes on V^{IV}-V^V electrode kinetics. It is likely that the effects on the V^{II}-V^{III} kinetics are similarly due to oxidation and reduction of surface functional groups. Obviously, the details of the effects are considerably different for V^{II}-V^{III} than for V^{IV}-V^V.

In comparing the effects, it is instructive to compare the potentials at which activation and deactivation effects occur for the two couples, V^{II}-V^{III} and V^{IV}-V^V. Anodic treatment of an electrode activates it for the V^{II}-V^{III} reaction but deactivates it for the V^{IV}-V^V reaction. However, the observed potential for V^{II}-V^{III} activation (∼0.2 V) is considerably less positive than that (∼1.0 V) for V^{IV}-V^V deactivation

[d]Curve A_{45} does not show a clear saturation effect as is seen for the other curves. Experiments were limited to potentials ≤1.6 V to avoid possible complications due to carbon corrosion.

Table IV. Comparison of the potentials $E_{1/2}$ for 50% activation and 50% deactivation (from Fig. 7) after the corresponding anodic and cathodic treatment of the electrodes indicated. Results are shown for both V^{II}-V^{III} and V^{IV}-V^{V}.

Electrode Material	V^{II}-V^{III} $E_{1/2}$ (V)		V^{IV}-V^{V} $E_{1/2}$ (V)	
	Activation (Anodization)	Deactivation (Cathodization)	Activation (Cathodization)	Deactivation (Anodization)
Glassy Carbon	0.1	−1.3	−0.3	0.9
Carbon Paper	0.4	−1.2	−0.2	1.0
Carbon Xerogel	0.3	−1.3	−0.1	1.1
Fiber	0.0	−1.3	−0.1	1.1
Average	0.2	−1.3	−0.2	1.0

(see Table IV). This strongly suggests that the nature of the oxidation process is significantly different in the two cases. Thus it is likely that the specific oxidized forms of the surface functional groups responsible for activating the V^{II}-V^{III} reaction are different from those responsible for deactivating the V^{IV}-V^{V} reaction. Likewise the observed potential at which cathodic treatment of an electrode deactivates it for V^{II}-V^{III} ($\sim$−1.3 V) is considerably more negative than that ($\sim$−0.2 V) which activates it for V^{IV}-V^{V}. Therefore, in this case also it is likely that the specific reduced forms of the surface functional groups responsible for activating V^{IV}-V^{V} are different from those responsible for deactivating V^{II}-V^{III}. Thus, the electrode state which enhances V^{II}-V^{III} is not equivalent to that which inhibits V^{IV}-V^{V} and the state which inhibits V^{II}-V^{III} is not equivalent to that which enhances V^{IV}-V^{V}.

It is, in fact, possible that enhancement of both V^{II}-V^{III} and V^{IV}-V^{V} is due to the same (active) state of the electrode. In that scenario, oxidation of this active state leads to inhibition for V^{IV}-V^{V} while reduction of the same active state leads to inhibition for V^{II}-V^{III}. The question then arises, of course, as to why inhibition of V^{IV}-V^{V} is not observed after strong cathodization of the electrode and why inhibition of V^{II}-V^{III} is not observed after strong anodization. The answer may be that the strongly reduced state cannot persist under the oxidizing conditions of the V^{IV}-V^{V} electrolyte and that the strongly oxidized state cannot persist under the reducing conditions of the V^{II}-V^{III} electrolyte. For example, it can be seen from Curve A$_{23}$ in Fig. 7 that a cathodized electrode, initially deactivated for V^{II}-V^{III}, is strongly activated by holding it at $\sim$0.46 V (the V^{IV}-V^{V} rest potential); thus, such an electrode would not remain inactive in a V^{IV}-V^{V} electrolyte long enough for the effect to be observed. Likewise, it can be seen from Curve C$_{45}$ in Fig. 7 that an anodized electrode, initially deactivated for V^{IV}-V^{V}, is strongly activated by holding it at $\sim$−0.9 V (the V^{II}-V^{III} rest potential); thus, such an electrode would not remain inactive in a V^{II}-V^{III} electrolyte long enough for the effect to be observed.

In summary, while cathodic treatment of carbon leads to inhibition of V^{II}-V^{III} and enhancement of V^{IV}-V^{V}, these two effects do not correspond to a common reduced state of the electrode. Likewise, while anodic treatment of carbon leads to enhancement of V^{II}-V^{III} and inhibition of V^{IV}-V^{V}, these two effects do not correspond to a common oxidized state of the electrode. It is possible that the state of the electrode responsible for enhancement of V^{II}-V^{III} is, in fact, similar to the state responsible for enhancement of V^{IV}-V^{V}.

Conclusions

It was shown for four different types of carbon that the kinetics of the V^{II}-V^{III} reaction is enhanced by anodic treatment of the electrode and inhibited by cathodic treatment. In contrast, the kinetics of the V^{IV}-V^{V} reaction is inhibited by anodic treatment of an electrode and enhanced by cathodic treatment. Both EIS and CV experiments showed that alternate cathodization and anodization of the electrode repeatedly and reproducibly toggled its behavior, affecting V^{II}-V^{III} and V^{IV}-V^{V} in opposite senses: anodization enhanced the kinetics of V^{II}-V^{III} but inhibited the kinetics of V^{IV}-V^{V} while cathodization had the opposite effects.

The effects of treatment potential on both V^{II}-V^{III} and V^{IV}-V^{V} were examined in detail for both anodization and cathodization. For V^{II}-V^{III}, anodic treatment at potentials in the region of $\sim$0.1 V caused

an increase in activity while cathodic treatment in the region of $\sim$−1.3 V caused a decrease in activity. Likewise but conversely for V^{IV}-V^{V}, anodic treatment in the region of $\sim$0.9 V caused a decrease in activity while cathodic treatment in the region of $\sim$−0.3 V caused an increase in activity. The potential region for each of these effects varied only slightly with carbon material and analysis technique.

The ATF (defined in the text) was estimated for each carbon material. For V^{II}-V^{III} the ATF was always > 1 as expected, ranging from 8.87 for carbon fiber to 24.6 for carbon paper. Likewise, for V^{IV}-V^{V} the ATF was always < 1, ranging from 0.104 for glassy carbon to 0.212 for carbon fiber. Because of the size of these effects, the primary finding of this paper is plain; i.e. that cathodization and anodization of the electrode affect V^{II}-V^{III} and V^{IV}-V^{V} in opposite senses.

The rate constants for V^{II}-V^{III} were compared with those for V^{IV}-V^{V} on each carbon. The comparison was complicated by the strong and contrasting effects of electrode treatment for the two systems. However, the observed rate constants were always greater for V^{IV}-V^{V} than for V^{II}-V^{III} except when anodized electrodes were compared; in the latter case, the normal trend could be reversed because anodization enhanced V^{II}-V^{III} and inhibited V^{IV}-V^{V}. These observations may explain discrepancies and inconsistencies in the literature. Further work needs to be done to more precisely characterize the kinetics and mechanism for each of the couples. However, it is now clear from our research that such studies will need to take careful account of the effects of electrode treatment.

It is suggested that oxygen-containing species, known to occur on the surface of carbon electrodes, are responsible for the observed effects of cathodic and anodic treatment. Obviously, the details of the effects are considerably different for V^{II}-V^{III} than for V^{IV}-V^{V}. While anodic treatment of carbon leads to enhancement of V^{II}-V^{III} and inhibition of V^{IV}-V^{V}, the considerable difference between the potentials at which these two effects occur indicates that they do not correspond to a common oxidized state of the electrode. Likewise while cathodic treatment of carbon leads to inhibition of V^{II}-V^{III} and enhancement of V^{IV}-V^{V}, the considerable difference between the potentials at which these two effects occur indicates that they do not correspond to a common reduced state of the electrode.

It is, in fact, possible that enhancement of both V^{II}-V^{III} and V^{IV}-V^{V} is due to the same (active) state of the electrode. In that scenario, oxidation of this active state leads to inhibition of V^{IV}-V^{V} while reduction of the same active state leads to inhibition of V^{II}-V^{III}. Inhibition of V^{IV}-V^{V} is not observed after strong cathodization possibly because the strongly reduced state may not be able to persist under the oxidizing conditions of the V^{IV}-V^{V} electrolyte; likewise inhibition of V^{II}-V^{III} is not observed after strong anodization possibly because the strongly oxidized state may not be able to persist under the reducing conditions of the V^{II}-V^{III} electrolyte.
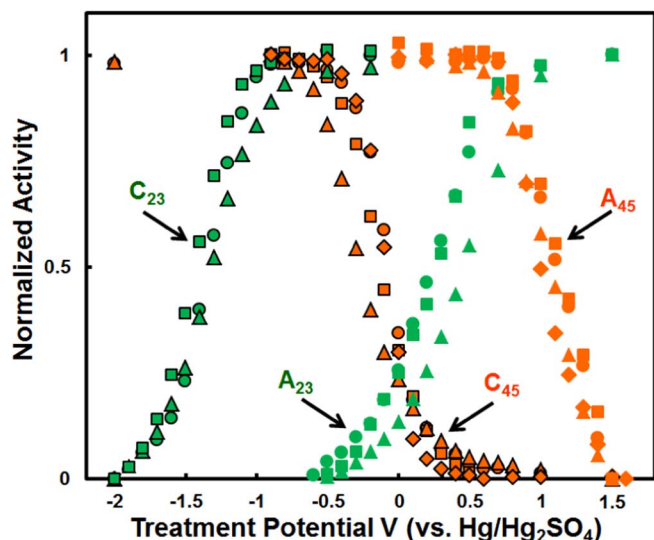
Figure A1. Normalized activity estimated from CV currents plotted against treatment potential for four types of carbon. Data for both anodic (A) and cathodic (C) treatments are shown for both V^{II}-V^{III} (A$_{23}$ and C$_{23}$) and V^{IV}-V^{V} (A$_{45}$ and C$_{45}$). The materials shown are: glassy carbon ●, carbon paper ▲, carbon xerogel ■, and carbon fiber ♦. Normalized activity is defined as $a = \frac{I - I_d}{I_a - I_d}$ where I is the CV current (as defined for Fig. 5) after treatment at a given potential; I_a and I_d are the currents after maximum activation and maximum deactivation, respectively. The experiments were carried out as described earlier for Figs. 5 and 6.

Appendix

CV results for effect of treatment potential.— The detailed effects of treatment potential on each of the four types of carbon were also investigated using CVs as the metric. The results are summarized in Fig. A1 where the normalized activity after both cathodic (C) and anodic (A) treatment is plotted against treatment potential for both V^{II}-V^{III} (C$_{23}$ and A$_{23}$) and V^{IV}-V^{V} (C$_{45}$ and A$_{45}$). In agreement with the EIS results in Fig. 7, it can be seen that all four carbons behave in a similar manner: in all cases, anodic treatment results in enhancement of V^{II}-V^{III} and inhibition of V^{IV}-V^{V} while cathodic treatment results in inhibition of V^{II}-V^{III} and enhancement of V^{IV}-V^{V}. Furthermore it can be seen that in each case (A$_{23}$, A$_{45}$, C$_{23}$, and C$_{45}$) activation or deactivation occurs over a similar range of potential for all four carbons.

The CV currents (as defined for Fig. 5) for both V^{II}-V^{III} and V^{IV}-V^{V} after maximum anodic treatment and maximum cathodic treatment are listed in Table A1 for all four carbons investigated. The ratio of the current after anodic treatment to that after cathodic treatment is also shown in each case. It can be seen that in all cases this ratio is >1 for V^{II}-V^{III}, ranging from 2.96 for carbon fiber to 7.25 for carbon paper. In contrast, in all cases the ratio is <1 for V^{IV}-V^{V}, ranging from 0.153 for glassy carbon to 0.547 for carbon xerogel.

Comparison of CVs obtained after treatment at −0.9 V and −2.0 V.— A CV obtained on a glassy-carbon electrode in V^{IV}-V^{V} electrolyte after treatment at −2.0 V (solid curve) is compared with that obtained after treatment at −0.9 V (dashed curve) in Fig. A2. It can be seen that there is very little difference in current between the two curves indicating that the activity of the electrode after cathodic treatment at −2.0 V is approximately the same as that after cathodic treatment at −0.9 V.
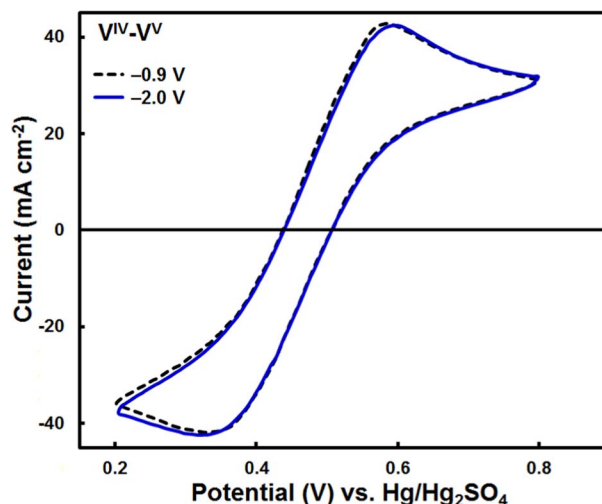

Figure A2. Comparison of CVs of a glassy-carbon electrode in a V^{IV}-V^{V} electrolyte after cathodic treatment at −2.0 V (solid line) and −0.9 V (broken line) for 60 s. The scan rate was 50 mV s^{-1}.

Comparison of V^{II}-V^{III} and V^{IV}-V^{V} using CVs.— Typical CV results on glassy carbon for V^{II}-V^{III} and V^{IV}-V^{V} are compared in Fig. A3. In each case a CV for both an anodized and a cathodized electrode is shown. Clearly, the currents for V^{IV}-V^{V} after cathodic activation (C$_{45}$) are greater than those for V^{II}-V^{III} after anodic activation (A$_{23}$). Likewise the currents for V^{IV}-V^{V} after anodic deactivation (A$_{45}$) are greater than those for V^{II}-V^{III} after cathodic deactivation (C$_{23}$).
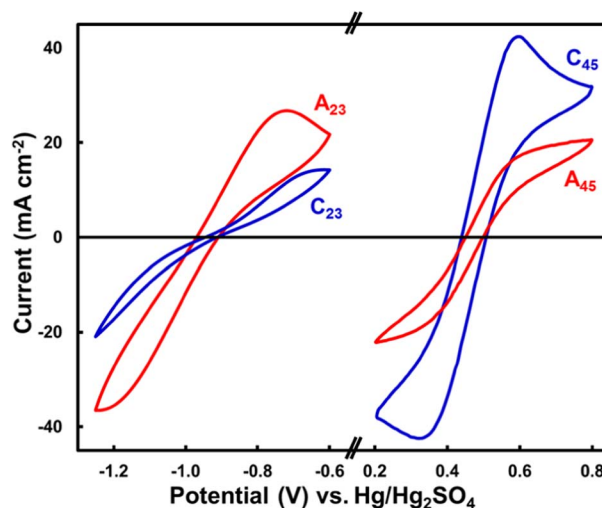

Figure A3. Comparison of the CV responses of V^{II}-V^{III} and V^{IV}-V^{V}. A$_{23}$ and C$_{23}$ correspond to V^{II}-V^{III} after, respectively, anodic and cathodic treatment of the electrode; similarly A$_{45}$ and C$_{45}$ correspond to V^{IV}-V^{V}. The data are from Fig. 2.

Table A1. Comparison of CV currents I_{cv} after maximum anodic treatment and maximum cathodic treatment for the electrodes indicated. The ratio of the CV current (as defined for Fig. 5) after anodic treatment I_{an} to that after cathodic treatment I_{cat} is also shown in each case. Results for both V^{II}-V^{III} and V^{IV}-V^{V} are shown (from Fig. 5 and Figs. 6, respectively, in the case of glassy carbon).

Electrode Material	V^{II}-V^{III}			V^{IV}-V^{V}		
	I_{an} (mA cm^{-2})	I_{cat} (mA cm^{-2})	I_{an}/I_{cat}	I_{an} (mA cm^{-2})	I_{cat} (mA cm^{-2})	I_{an}/I_{cat}
Glassy carbon	7.06	1.53	4.61	7.40	21.0	0.352
Carbon Paper	1.16	0.16	7.25	2.44	7.17	0.340
Carbon Xerogel	13.5	2.72	4.96	14.5	26.5	0.547
Fiber	2.40	0.81	2.96	1.73	11.3	0.153

References

1. M. J. Leahy, D. Connolly, and D. N. Buckley, *Wind Energy Storage Technologies in Wind Power Generation and Wind Turbine Design*, W. Tong, Editor, WIT Press, Southampton, (2009), p. 661.
2. M. H. Chakrabarti, N. P. Brandon, S. A. Hajimolana, F. Tariq, V. Yufit, M. A. Hashim, M. A. Hussain, C. T. J. Low, and P. V. Aravind, *Journal of Power Sources*, **253**, 150 (2014).
3. A. Z. Weber, M. M. Mench, J. P. Meyers, P. N. Ross, J. T. Gostick, and Q. Liu, *Journal of Applied Electrochemistry*, **41**, 1137 (2011).
4. A. Parasuraman, T. M. Lim, C. Menictas, and M. Skyllas-Kazacos, *Electrochimica Acta*, **101**, 27 (2013).
5. M. Skyllas-Kazacos, M. H. Chakrabarti, S. A. Hajimolana, F. S. Mjalli, and M. Saleem, *Journal of The Electrochemical Society*, **158**, R55 (2011).
6. C. Ponce de León, A. Frías-Ferrer, J. González-García, D. A. Szánto, and F. C. Walsh, *Journal of Power Sources*, **160**, 716 (2006).
7. M. Vynnycky, *Energy*, **36**, 2242 (2011).
8. G. Kear, A. A. Shah, and F. C. Walsh, *International Journal of Energy Research*, **36**, 1105 (2012).
9. M. J. Watt-Smith, P. Ridley, R. G. A. Wills, A. A. Shah, and F. C. Walsh, *Journal of Chemical Technology and Biotechnology*, **88**, 126 (2013).
10. C. Petchsingh, N. Quill, J. T. Joyce, D. Ní Eidhin, D. Oboroceanu, C. Lenihan, X. Gao, R. P. Lynch, and D. N. Buckley, *Journal of the Electrochemical Society*, **163**, A5068 (2016).
11. D. N. Buckley, X. Gao, R. P. Lynch, N. Quill, and M. J. Leahy, *Journal of The Electrochemical Society*, **161**, A524 (2014).
12. D. N. Buckley, X. Gao, R. P. Lynch, M. J. Leahy, A. Bourke, and G. Flynn, European Pat. EP 13195315, (2013); N. Quill, C. Petchsingh, R. P. Lynch, X. Gao, D. Oboroceanu, D. Ní Eidhin, M. O'Mahony, C. Lenihan, and D. N. Buckley, *ECS Transactions*, **64**, 23 (2015).
13. X. Gao, R. P. Lynch, M. J. Leahy, and D. N. Buckley, *ECS Transactions*, **45**, 25 (2013).
14. X. Gao, A. Bourke, R. P. Lynch, M. J. Leahy, and D. N. Buckley, *Conference Papers The International Flow Battery Forum* **2013**, 20 (2013).
15. Z. Tang, D. S. Aaron, A. B. Papandrew, and T. A. Zawodzinski, *ECS Transactions*, **41**, 1 (2012).
16. M. Skyllas-Kazacos and M. Kazacos, *Journal of Power Sources*, **196**, 8822 (2011).
17. N. Quill, R. P. Lynch, X. Gao, and D. N. Buckley, *The Electrochemical Society Meeting Abstract*, **MA2014-01**, 389 (2014).
18. A. H. Whitehead and M. Harrer, *Journal of Power Sources*, **230**, 271 (2013).
19. F. Rahman and M. Skyllas-Kazacos, *Journal of Power Sources*, **189**, 1212 (2009).
20. M. Vijayakumar, W. Wang, Z. Nie, V. Sprenkle, and J. Hu, *Journal of Power Sources*, **241**, 173 (2013).
21. H. Prifti, A. Parasuraman, S. Winardi, T. M. Lim, and M. Skyllas-Kazacos, *Membranes*, **2**, 275 (2012).
22. A. Bourke, M. A. Miller, R. P. Lynch, J. S. Wainright, R. F. Savinell, and D. N. Buckley, *Journal of The Electrochemical Society*, **162**, A1547 (2015).
23. A. Bourke, M. A. Miller, R. P. Lynch, J. S. Wainright, R. F. Savinell, and D. N. Buckley, *ECS Transactions*, **66**, 181 (2015).
24. A. Bourke, R. P. Lynch, and D. N. Buckley, *ECS Transactions*, **64**, 1 (2015).
25. A. Bourke, N. Quill, R. P. Lynch, and D. N. Buckley, *ECS Transactions*, **61**, 15 (2014).
26. A. Bourke, N. Quill, R. P. Lynch, and D. N. Buckley, *Conference Papers The International Flow Battery Forum 2014*, 16 (2014).
27. A. Bourke, R. P. Lynch, and D. N. Buckley, *ECS Transactions*, **53**, 59 (2013).
28. G. Oriji, Y. Katayama, and T. Miura, *Journal of Power Sources*, **139**, 321 (2005).
29. E. Sum and M. Skyllas-Kazacos, *Journal of Power Sources*, **15**, 179 (1985).
30. E. Sum, M. Rychcik, and M. Skyllas-Kazacos, *Journal of Power Sources*, **16**, 85 (1985).
31. D. Aaron, C.-N. Sun, M. Bright, A. B. Papandrew, M. M. Mench, and T. A. Zawodzinski, *ECS Electrochemistry Letters*, **2**, A29 (2013).
32. C.-N. Sun, F. M. Delnick, D. S. Aaron, A. B. Papandrew, M. M. Mench, and T. A. Zawodzinski, *ECS Electrochemistry Letters*, **2**, A43 (2013).
33. J. W. Lee, J. K. Hong, and E. Kjeang, *Electrochimica Acta*, **83**, 430 (2012).
34. M. Gattrell, J. Park, B. MacDougall, J. Apte, S. McCarthy, and C. W. Wu, *Journal of The Electrochemical Society*, **151**, A123 (2004).
35. H. Kaneko, K. Nozaki, Y. Wada, T. Aoki, A. Negishi, and M. Kamimoto, *Electrochimica Acta*, **36**, 1191 (1991).
36. A. Di Blasi, O. Di Blasi, N. Briguglio, A. S. Aricò, D. Sebastián, M. J. Lázaro, G. Monforte, and V. Antonucci, *Journal of Power Sources*, **227**, 15 (2013).
37. W. Li, J. Liu, and C. Yan, *Carbon*, **55**, 313 (2013).
38. W. Zhang, J. Xi, Z. Li, H. Zhou, L. Liu, Z. Wu, and X. Qiu, *Electrochimica Acta*, **89**, 429 (2013).
39. J. Xi, W. Zhang, Z. Li, H. Zhou, L. Liu, Z. Wu, and X. Qiu, *International Journal of Electrochemical Science*, **8**, 4700 (2013).
40. Y. Men and T. Sun, *International Journal of Electrochemical Science*, **7**, 3482 (2012).
41. X. G. Li, K. L. Huang, S. Q. Liu, N. Tan, and L. Q. Chen, *Transactions of Nonferrous Metals Society of China (English Edition)*, **17**, 195 (2007).
42. M. A. Miller, R. F. Savinell, and J. S. Wainright, *The Electrochemical Society Meeting Abstract*, **MA2014-02**, 25 (2014).
43. L. Yue, W. Li, F. Sun, L. Zhao, and L. Xing, *Carbon*, **48**, 3079 (2010).
44. B. Sun and M. Skyllas-Kazacos, *Electrochimica Acta*, **37**, 2459 (1992).
45. E. Agar, C. R. Dennison, K. W. Knehr, and E. C. Kumbur, *Journal of Power Sources*, **225**, 89 (2013).
46. J. Friedl, C. Bauer, A. Rinaldi, and U. Stimming, *Carbon*, **63**, 228 (2013).
47. B. Sun and M. Skyllas-Kazacos, *Electrochimica Acta*, **37**, 1253 (1992).
48. Z. González, C. Botas, P. Álvarez, S. Roldán, C. Blanco, R. Santamaría, M. Granda, and R. Menéndez, *Carbon*, **50**, 828 (2012).
49. C. Flox, J. Rubio-García, M. Skoumal, T. Andreu, and J. R. Morante, *Carbon*, **60**, 280 (2013).
50. X. W. Wu, T. Yamamura, S. Ohta, Q. X. Zhang, F. C. Lv, C. M. Liu, K. Shirasaki, I. Satoh, T. Shikama, D. Lu, and S. Q. Liu, *Journal of Applied Electrochemistry*, **41**, 1183 (2011).
51. T. Yamamura, N. Watanabe, T. Yano, and Y. Shiokawa, *Journal of The Electrochemical Society*, **152**, A830 (2005).
52. P. Chen, M. A. Fryling, and R. L. McCreery, *Analytical Chemistry*, **67**, 3115 (1995).
53. M. Gattrell, J. Qian, C. Stewart, P. Graham, and B. MacDougall, *Electrochimica Acta*, **51**, 395 (2005).
54. K. J. Kim, Y. J. Kim, J. H. Kim, and M. S. Park, *Materials Chemistry and Physics*, **131**, 547 (2011).
55. W. Li, J. Liu, and C. Yan, *Electrochimica Acta*, **79**, 102 (2012).
56. S. Zhong and M. Skyllas-Kazacos, *Journal of Power Sources*, **39**, 1 (1992).
57. K. Kinoshita, *Carbon: Electrochemical and Physicochemical Properties*, Wiley, New York, (1988).
58. G. M. Swain, *Solid Electrode Materials: Pretreatment and Activation* C. G. Zoski, Editor, Elsevier, Amsterdam, (2007), p. 111.
59. K. R. Kneten and R. L. McCreery, *Analytical Chemistry*, **64**, 2518 (1992).
60. R. C. Engstrom, *Analytical Chemistry*, **54**, 2310 (1982).
61. C. McDermott, K. Kneten, and R. McCreery, *Journal of the Electrochemical Society*, **140**, 3 (1993).
62. F. Chen, J. Liu, H. Chen, and C. Yan, *International Journal of Electrochemical Science*, **7**, 3750 (2012).
63. Y. Shao, X. Wang, M. Engelhard, C. Wang, S. Dai, J. Liu, Z. Yang, and Y. Lin, *Journal of Power Sources*, **195**, 4375 (2010).
64. X. Gao, A. Omosebi, J. Landon, and K. Liu, *Energy & Environmental Science*, **8**, 897 (2015).
65. X. Gao, A. Omosebi, J. Landon, and K. Liu, *Electrochemistry Communications*, **39**, 22 (2014).
66. X. Gao, J. Landon, J. K. Neathery, and K. Liu, *Journal of The Electrochemical Society*, **160**, E106 (2013).
67. J. Landon, X. Gao, B. Kulengowski, J. K. Neathery, and K. Liu, *Journal of The Electrochemical Society*, **159**, A1861 (2012).
68. A. J. Bard and L. R. Faulkner, *Electrochemical Methods: Fundamentals and Applications*, Wiley, New York, (2000).
69. L. Otero, N. Vettorazzi, and L. Sereno, *Journal of The Electrochemical Society*, **148**, E413 (2001).
70. M. Noel and P. N. Anantharaman, *Analyst*, **110**, 1095 (1985).
71. G. E. Cabaniss, A. A. Diamantis, W. R. Murphy, R. W. Linton, and T. J. Meyer, *Journal of the American Chemical Society*, **107**, 1845 (1985).
72. G. Ilangovan and K. Chandrasekara Pillai, *Langmuir*, **13**, 566 (1997).